Numerical and Dynamical Analyses of Heat Source Forcing and Restricting Subtropical High Activity①

Zhang Ren (张 韧) and Yu Zhihao (余志豪)

Department of Atmospheric Science, Nanjing University, Nanjing 210093

(Received January 8, 1999; revised August 10, 1999)

ABSTRACT

By using the numerical and dynamical methods, the influence and restriction of the heat source forcing on the subtropical geopotential fields and flow fields are studied and discussed in a model atmosphere. The main results show that the zonal symmetrical solar radiation heating chiefly induces the geopotential field changing gradually and leads the subtropical high moving slowly, but when the zonal asymmetric thermal difference between ocean and continent achieves its critical value, which usually causes the geopotential field a catastrophe, and consequently induces the subtropical high shake-up or jump. The abnormal activity of the subtropical high is possibly caused by the abnormality of the thermal factor.

Key words: Subtropical high, Thermal forcing

1. Introduction

The West Pacific subtropical high (WPSH) is a main system influencing the weather and climate of East Asia in summer, whose intensity variation and advance / retreat are closely related to the cool / warm of weather and the plenty / defficiency of precipitation of this region in summer. In history, the flood and drought in East Asia greatly depend on the abnormality of WPSH, for example, the serious drought / flood in the summer of 1959 and 1998. Recently, there are many researches about WPSH, the seasonal jump and catastrophe mechanism of WPSH was also studied and discussed from dynamic viewpoints, and some useful results were obtained (Liu et al., 1983; Miao et al., 1985). But the functional rule of WPSH is not made clear yet, especially, the medium-range advance / retreat and abnormal variation mechanism of WPSH is still waiting for being further revealed. Charney (1979) once studied the blocking pattern and equilibrium state of the middle / high latitude atmospheric circulation using the dynamical method of the high truncated spectrum expanding, and made an innovational work in this field. The West Pacific subtropical high is a relatively stable large-scale weather body in the middle / low latitude atmospheric circulation, which is characterized with relatively long life cycle and gradual-change / catastrophe phenomena, the characteristics of WPSH mentioned above resemble the blocking pattern of the middle / high latitude atmospheric circulation. Therefore, we plan to study the WPSH system using the similar ways and means, by discussing the introduced several sorts of heat sources, the potential influence and restriction exerted on WPSH by different heat source patterns and heating intensity will be analyzed and studied. Based on the dynamical framework, for the problems

①Supported by National Natural Science Foundation (No. 49975012) and National ' 973' Key Program (No. G1998040907).

mentioned above the numerical calculation and the numerical simulation will be carried out in a model atmosphere. Through these researches, the medium-range advance / retreat and the abnormal movement rules or mechanism of WPSH in summer are expected to be understood and revealed in a certain extent.

2. Dynamical model

A non-linear barotropic vorticity equation with forcing / dissipation terms is adopted

$$\frac{\partial}{\partial t}(\nabla^2\psi)+ J(\psi,\nabla^2\psi)+ \beta\frac{\partial\psi}{\partial x} = - Q+ v\nabla^4\psi, \tag{1}$$

where ψ is the stream function, v is the horizontal vorticity diffusion coefficient, Q is a forcing term, which is vortex source (sink) produced by diabatic heating. Making the following transformation:

$$(x,y)\sim L_0(x',y'),\ t\sim\frac{1}{f_0}t',\ \psi\sim\frac{L_0^2}{T_0}\psi'\sim L_0^2 f_0\psi',\ Q\sim Q_0Q',$$

Equation (1) becomes a non-dimensional equation

$$\frac{\partial}{\partial t}(\nabla^2\psi)+ J(\psi,\nabla^2\psi)+ \bar{\beta}\frac{\partial\psi}{\partial x} = - \bar{Q}Q+ \bar{k}\nabla^4\psi, \tag{2}$$

where $\bar{\beta}=\frac{\beta_0 L_0}{f_0}$, $\bar{Q}=\frac{Q_0}{f_0^2}$, $\bar{k}=\frac{\varphi}{L_0^2 f_0}$.

Boundary conditions: The fixed-wall boundary condition $v=\left.\frac{\partial\psi}{\partial x}\right|_{y=\pm\frac{\pi}{2}}=0$ is taken for y-direction and periodic variation with 2π is taken for x-direction, the research region is defined as $D=\{x:0\leqslant x\leqslant 2\pi,\ y:-\pi/2\leqslant y\leqslant\pi/2\}$. Using the high truncated spectrum method, the following three maturity-normal fiducial functions are introduced:

$$f_1=\sqrt{2}\sin(2y),\ f_2=2\cos(y)\sin(2x),\ f_3=2\cos(2y)\cos(2x).$$

ψ and Q are expanded as $\psi=\psi_1(t)f_1+\psi_2(t)f_2+\psi_3(t)f_3$, $Q=Q_1f_1+Q_2f_2+Q_3f_3$.
The distribution of Q suggests: when $Q_1>0$, it means that the Northern Hemisphere is heated and the Southern Hemisphere is cooled in summer (contrariwise, when $Q_1<0$); when $Q_2>0$, it means that the northern hemispherical mainland is heated and ocean is cooled in summer (the zonal two-wave pattern can approximately reflect the geographical frame of two mainlands and two oceans in the Northern Hemisphere), Q_3 can be used to indicate the heating effect produced by the interaction between the meridional and zonal two waves.

These expressions mentioned above are introduced into Equation (2), then the partial differential equation can be transformed into an ordinary differential system, by multiplying the factors of f_1,f_2,f_3 and making integration over the region $D(x\in[0,2\pi],\ y\in[-\pi/2,\pi/2])$, then the ordinary differential equations can be obtained as follows:

$$\frac{d\psi_1(t)}{dt}=2.521\psi_2\psi_3+0.25\bar{Q}Q_1-4\bar{k}\psi_1, \tag{3}$$

$$\frac{d\psi_2(t)}{dt}=-2.689\psi_1\psi_3-0.17\bar{\beta}\psi_3+0.2\bar{Q}Q_2-5\bar{k}\psi_2, \tag{4}$$

$$\frac{d\psi_3(t)}{dt} = 0.42\psi_1\psi_2 + 0.106\bar{\beta}\psi_2 + 0.125\bar{Q}Q_3 - 7.998\bar{k}\psi_3. \tag{5}$$

Next, we will make numerical calculation and dynamical analysis of this weather model.

3. Numerical simulation of different heat source patterns

Taking $f_0 = 5.0\times 10^{-5}s^{-1}$, $\beta_0 = 2.15\times 10^{-11}m^{-1}s^{-1}$ (about 20°N) $L_0 = 10^6$ m, $Q_0 = 1.0\times f_0^2 s^{-2}$, $\nu = 3.5\times 10^6 m^2 s^{-1}$, the 4/5 step Runge–Kutta method with different step length is adopted to perform numerical integration for equations (3)–(5). If 1 h is taken as integral step length, and the equations are integrated for 30 days, we find that different heat source patterns will make different contributions to the integral results of ψ. If the initial condition is taken as $[\psi_1, \psi_2, \psi_3]_0 = [0,0,0]$, and the seasonal solar heating ($Q_1 = 0.3$) and a marked thermal difference between sea and land ($Q_2 = 0.7$) are considered, the numerical simulation of ψ_1, ψ_2, ψ_3 is obtained as Fig. 1.

From Fig.1, it is shown that the stream function field (geopotential field) increases clearly from the initial zero point and maintains in a stable position after being integrated 10 days, which indicates that under the above thermal forcing, the stream function field (geopotential field) will have an evident development and jump to a high geopotential state from its original low geopotential state.

The integral results of Fig. 2 show that if the thermal difference between sea and land is not considered ($Q_2 = 0$) and only seasonal solar heating is taken, within the calculation results shown in Fig. 2, only the 1st mode of ψ increases obviously, and the 2nd as well as 3rd mode hardly change with time. Because this increase of the 1st mode is a common state centred in middle latitudes in the Northern Hemisphere, which expresses a regular seasonal change process of the stream field and the geopotential field in the Northern Hemisphere. From the fiducial function pattern of the 1st mode, we can see that this sort of change of ψ_1 cannot represent the longitudinal pattern of the stream field and the geopotential field and also cannot express the geographical distribution characteristics of the stream field and the

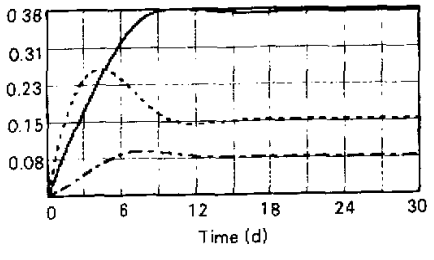

Fig. 1. The numerical integral of ψ_1 (solid), ψ_2 (dashed), ψ_3 (dot–dashed) when $Q_1 = 0.3, Q_2 = 0.7, Q_3 = 0.1$.

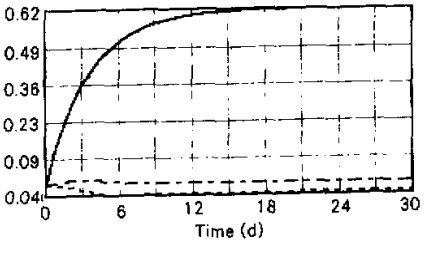

Fig. 2. The same as in Fig. 1.

geopotential field with the zonal sea / land difference, as a result, it cannot represent the complex and irregular development process of regional weather system (such as WPSH). If a marked thermal difference between sea and land is considered ($Q_2 = 0.7$), and the seasonal solar heating is omitted ($Q_1 = 0$), taking $Q_3 = 0.1$, the numerical integral of every ψ's mode will have an evident growth (figure omitted). Because of the interaction between different modes and the longitudinal and zonal characteristic pattern of the fiducial function, the group combined by different ψ's modes can represent various development processes of stream field and geopotential field in different areas of the Northern Hemisphere, and can describe the relatively complicated weather patterns and movement model, including WPSH.

If the seasonal solar heating (taking $Q_1 = 0.3$), the thermal difference between sea and land (taking $Q_2 = 0.7$) and a larger thermal factor Q_3 (taking $Q_3 = 0.7$) are synchronously introduced, the integral results of the 1st and 2nd modes of ψ are similar to Fig. 1, viz. the thermal factor Q_3 does not have a marked influence on mode 1 and mode 2 of ψ, moreover, mode 3 is slightly weaken in the case of considering Q_3 (figure omitted).

Summing up what were discussed above, within the thermal factors inducing the stream field and the geopotential field change, the effects of terms Q_1 and Q_2 are outstanding but that of term Q_3 is weak. From the distribution meaning of Q, the seasonal solar heating (Q_1) and the thermal difference between sea and land (Q_2) are the key factors inducing the stream field ψ as well as the geopotential field φ (for $\varphi \approx g \cdot \psi$) change, comparing Q_2 with Q_1, the effect, inducing the weather system development, of the former is greater than that of the latter.

4. Equilibrium state and bifurcation

For the large–scale weather systems (such as WPSH), when they are in a quasi–stationary state, the time–varied terms of their dynamic model are small values, then the left terms of equations (3)~(5) can be taken as zero, therefore, the equilibrium state equations describing this sort of weather phenomena are as follows:

$$2.521\psi_2\psi_3 + 0.25\bar{Q}Q_1 - 4\bar{k}\psi_1 = 0, \tag{6}$$

$$-2.689\psi_1\psi_3 - 0.17\bar{\beta}\psi_3 + 0.2\bar{Q}Q_2 - 5\bar{k}\psi_2 = 0, \tag{7}$$

$$0.42\psi_1\psi_2 + 0.106\bar{\beta}\psi_2 + 0.125\bar{Q}Q_3 - 7.998\bar{k}\psi_3 = 0. \tag{8}$$

By discussing the variation and equilibrium point pattern of this equilibrium system, the evolution of the quasi–stationary system (such as WPSH) with thermal forcing can be expressed. By using the numerical calculation method, the evolution process of the equilibrium points changing with thermal parameters Q_1, Q_2, Q_3 can be represented. Setting $Q_1 = 0.3$ and $Q_3 = 0.1$, the evolution process of $\bar{\psi}_2$ changing with Q_2 is as Fig. 3.

From Fig. 3, it is shown that a bifurcation of $\bar{\psi}_2$ appears when Q_2 increases to about 0.6, and a single–resolution state becomes a three–resolution state. In other words, the weather system changes into a multi–equilibrium state from a single–equilibrium state when

Q_2 increases from a low value ($Q_2 < 0.6$) to a high value ($Q_2 > 0.6$), where the bifurcation point is about 0.6, and two resolutions of the system present a marked jump near the bifurcation point. By analyzing the stability of the equilibrium points, it is shown that the single-equilibrium resolution before bifurcation is stable, but, within the multi-equilibrium resolutions after bifurcation, $\overline{\psi}_{21}$ is stable, and $\overline{\psi}_{22}$, $\overline{\psi}_{23}$ are unstable, which suggests that the system will jump to a stable high-equilibrium state from a stable low-equilibrium state when the thermal forcing factor Q_2 exceeds a certain critical value. For the subtropical high system, the process of ψ jumping from a low-geopotential mode to a high-geopotential mode will be likely shown as a "catastrophe" of WPSH.

Taking $Q_2 = 0.7$ and $Q_3 = 0.1$, the variation of $\overline{\psi}_1$ with Q_1 is described as Fig. 4. From Fig. 4, it is shown that the critical point between the single-equilibrium state and the multi-equilibrium state is located at about 0.5 (between 0.4 and 0.5), where three equilibrium solutions jump into a single-equilibrium solution. Stability analysis of the equilibrium states shows that the 2nd ($\overline{\psi}_{12}$ ——) and 3rd ($\overline{\psi}_{13}$ – · –) equilibrium states are unstable, and the 1st ($\overline{\psi}_{11}$ ——) equilibrium state is stable. From what were discussed above, it is suggested that, under the condition that thermal factors Q_2,Q_3 keep constant, the variation of $\overline{\psi}_1$ changing with Q_1 is gradual, which reflects that in the area centred in middle latitudes of the Northern Hemisphere, the enhancement of stream field and geopotential field induced by the seasonal solar heating is a gradual process.

Summing up the above analyses, among the thermal factors influencing the summer stream field and geopotential field in the northern hemispherical subtropical area, generally speaking, Q_1 is likely a gradual-variation factor, viz., the seasonal solar heating mainly induces WPSH enhancing gradually or moving slowly; whereas, Q_2 is likely a catastrophic factor, viz., the thermal difference produced by cross-pattern of the northern hemispherical sea and land (e.g. land heating and sea cooling in summer) is likely a main factor inducing WPSH catastrophe or circulation abnormality. Q_3 is a heating effect produced by the interaction between waves, which is only a minor influence factor for the large scale weather systems, such as WPSH.

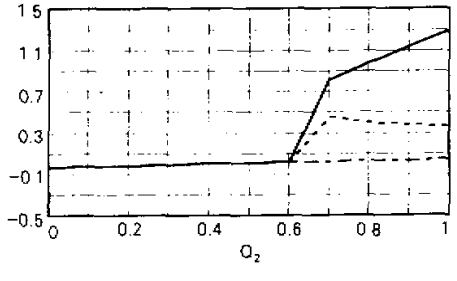

Fig. 3. The pattern between equilibrium point $\overline{\psi}_2$ ($\overline{\psi}_{21}$ ——, $\overline{\psi}_{22}$ ——, $\overline{\psi}_{23}$ – · –) and thermal factor Q_2.

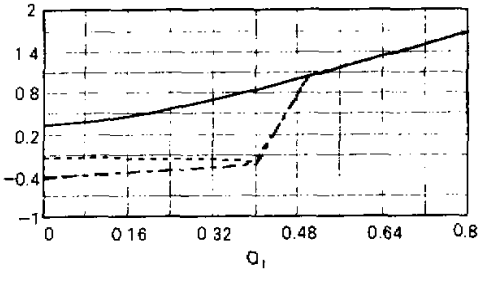

Fig. 4. The pattern between equilibrium point $\overline{\psi}_1$ ($\overline{\psi}_{11}$ ——, $\overline{\psi}_{12}$ ——, $\overline{\psi}_{13}$ – · –) and thermal factor Q_1.

5. Numerical simulation of stream and geopotential field

Taking $u = -\frac{\partial \psi}{\partial y}$, $v = \frac{\partial \psi}{\partial x}$ and $\varphi = g \cdot \psi$, then

$$u(x,y) = -2\sqrt{2} \cdot \cos(2 \cdot y) \cdot \psi_1 + 2\sin(y) \cdot \sin(2 \cdot x) \cdot \psi_2 + 4\sin(2 \cdot y) \cdot \cos(2 \cdot x) \cdot \psi_3,$$

$$v(x,y) = 4 \cdot \cos(y) \cdot \cos(2 \cdot x) \cdot \psi_2 - 4\cos(2 \cdot y) \cdot \sin(2 \cdot x) \cdot \psi_3,$$

$$\varphi(x,y) = 9.8(\sqrt{2} \cdot \psi_1 \cdot \sin(2 \cdot y) + 2 \cdot \psi_2 \cdot \cos(y) \cdot \sin(2 \cdot x) + 2 \cdot \psi_3 \cos(2 \cdot y) \cdot \cos(2 \cdot x)).$$

Setting initial values: $\psi_1 = 0.6$, $\psi_2 = -0.7$, $\psi_3 = 0.15$, then the initial stream field (Fig. 5) and the initial geopotential field (omitted) of the northern hemispherical model atmosphere are obtained.

It can be seen from Fig. 5 that there are two evident anticyclone centers (subtropical high center) over the subtropical ocean between 22.5°N and 45°N (the Northern Hemisphere is simply divided into two lands ($0 \sim \frac{\pi}{2}$, $\pi \sim \frac{3\pi}{2}$) and two oceans ($\frac{\pi}{2} \sim \pi$, $\frac{3\pi}{2} \sim 2\pi$) in model atmosphere), and two weak cyclone circulations (low pressure system) over the subtropical

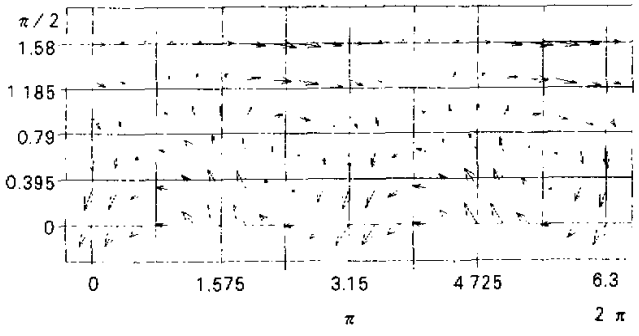

Fig. 5. Initial stream field of the northern hemispherical model atmosphere.

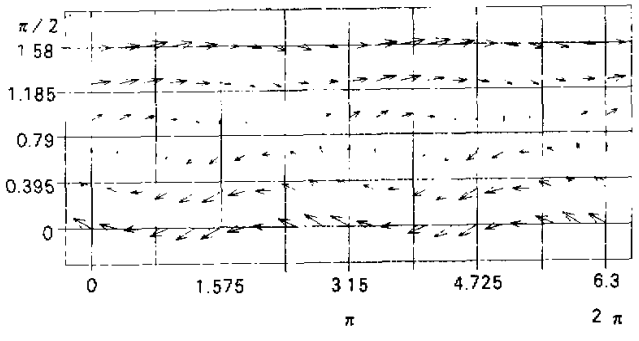

Fig. 6. The numerically simulated stream field of model atmosphere after integrating 15 days.

mainland. This ideal initial field of the model atmosphere defined above can approximately express the actual basic circulation structure and weather characteristics (the thermal forcing is weak and WPSH does not strengthen and extend eastward) of the Northern Hemisphere in early summer. Under the initial conditions, we introduce following thermal forcing: $Q_1 = 0.3$, $Q_2 = 0.7$, $Q_3 = 0.1$, and 4/5 step Runge–Kutta method with different step length is adopted to make numerical integral for Equations (3)–(5). If 1h is taken as the integral step length, and the equations are integrated for 15 days, the numerically simulated stream field is shown in Fig.6.

With the comparison between Fig. 5 and Fig.6, we can clearly find that after a period of sustained heating, all the stream fields and geopotential fields over the subtropical area have an outstanding change: the original weak cyclone low pressure system over the subtropical mainland is replaced by a whole anticyclone high pressure system, whereas the original strong subtropical high system over the oceans is clearly weakened. Because only a simple dynamic model is adopted, the numerical calculation results are comparatively ideal, and there are some differences from the actual condition (e.g. the subtropical high over the mainland is too strong, whose position is too westward and the subtropical high over the ocean is too weak and so on), but such results still can be obtained as follows: the collective effects of the thermal factors discussed in the model can induce the geopotential field over the subtropical mainland enhancing markedly, consequently, which is shown as that the subtropical high over the ocean extends westward/northward and moves toward the East Asian mainland, where the forcing effect produced by the zonal thermal difference between sea and land plays a more important role.

6. Numerical experiment of heat source influencing WPSH

In order to check (investigate) whether the thermal factors introduced in our model can reflect the actual normal weather seasonal variation and to discuss the possible influence on the subtropical high produced by abnormal heating, a seasonal heating term and an abnormal heating term are respectively introduced into our model, and the relevant numerical experiments are also made respectively.

6.1 *Introduction of a periodic annual–variation heat source*

A periodic annual–variation heat source is introduced: $Q_{1t} = Q_1 \cdot \sin(\frac{2\pi}{T} \cdot t)$, $Q_{2t} = Q_2 \cdot \sin(\frac{2\pi}{T} \cdot t)$ and $Q_{3t} = Q_3 = 0.1$, where $T = 360$ days, $Q_1 = 0.3$ and $Q_2 = 0.7$, whose pattern is shown in Fig. 7.

Replacing the stationary heat source of Equations (3)–(5) with the periodic heat source defined above and integrating 360 days, then the annual variation pattern of every component of ψ with heat source is shown in Fig. 8.

Suppose that in the Northern Hemisphere the period of maximum heating effect is July (the corresponding integral time is the 90th day in the model) and the period of minimum heating effect is January (the corresponding integral time is the 270th day in the model), then we can see from Fig.8 that the variation of mode 1 (ψ_1) of ψ is roughly identical with the variation trend of thermal factor, viz, as the Northern Hemisphere is gradually heated or cooled, ψ_1 also increases gradually and reaches its maximum in July or weakens gradually and reaches its minimum in January. It is further shown that what the mode 1 of ψ represents

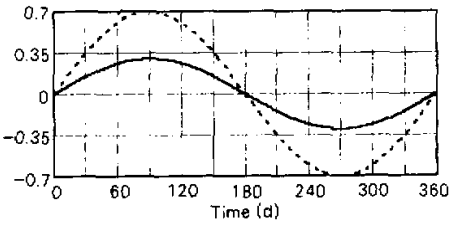

Fig. 7. Periodic annual heat source pattern. The solid and dashed lines are for Q_{1_t} and Q_{2_t} respectively.

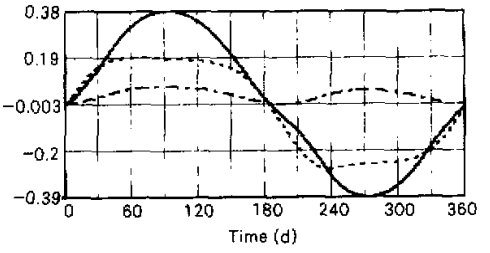

Fig. 8. Annual variation of every component of ψ ($—\psi_1, - - -\psi_2, - \cdot -\psi_3$) under the periodic thermal forcing.

is only such weather facts that the stream (geopotential) field is continuously / slowly changing with seasons, which can be used to reveal the basic character of WPSH strengthening and moving gradually with seasons. The time variation of mode 2 (ψ_2) of ψ is different from that of mode 1, and from its distribution curve, it is shown that the time of ψ_2 reaching its maximum and minimum is not in July (with maximum heat effect) and January (with minimum heat effect), whereas, there are an evidently increasing process and an obviously weakening process in March–May (the 330th–30th model days) and September–November (the 150th–210th model days) respectively, later on, during May–September and November–March, ψ_2 maintains a relatively smooth positive / negative value state respectively. The variation of mode 2 of ψ accords with the "May catastrophe" and the "October catastrophe" existed in the actual atmospheric circulation, which reflects such a weather fact: after the "May catastrophe" and the "October catastrophe", the circulation over the subtropical area comes into the summer circulation pattern and the winter circulation pattern respectively, at the same time, which also further verifies that under a continuous thermal forcing, the stream (geopotential) field of mode 2 of ψ has a sort of 'catastrophic' character. This dynamic character of ψ_2 can be briefly used to explain the seasonal 'northward–jump' phenomenon of WPSH in summer: when the solar heating and the thermal difference between sea and land increase gradually and reach their critical value, a catastrophe likely happens, and the stream (geopotential) field of synoptic system will jump into a high geopotential state from a low one, which is exhibited as WPSH suddenly intensifying and extending northward, after that, WPSH will maintain a relatively stable state (equilibrium state); when the thermal forcing increases continuously to its another critical value or when the thermal forcing decreases gradually back to its original critical value, the equilibrium state will lose its stability and another catastrophe likely happens, and the weather system likely jumps into a higher geopotential state or withdraws back to a lower geopotential state, consequently, which is represented as WPSH secondly jumping northward or quickly withdrawing southward.

6.2 *Introduction of a seasonal abnormal heat source*

For the weather of East Asian area in summer, it is very important to discuss the possible

influence on WPSH induced by the abnormality of heat source. In the summer of 1998, an exceptionally rainstorm and serious flood occurred in the Yangtze River valley, one main reason of this calamity is that after coming out of the meiyu in early July, the WPSH's ridge line had moved to its normal climate position about 30°N, and under general condition, the WPSH's ridge line does not decline and retreat southward until August, but in the midsummer of 1998, one rare "retreating-southward" course was experienced from the mid July to the early August, and the extent of retreating-southward nearly reached 10 degrees (30–20°N) about 25 July. By investigating the reason, we can find that during the summer of 1998, the West Pacific "warm pool" had experienced an unusual thermal transformation course from a weak thermal state (El Nino period) to a strong thermal state (La Nina period). If the seasonal solar heating (Q_{1t}) over the East Asian mainland in the summer of 1998 is considered as normal, because of the quick thermal transfer course of the West Pacific "warm pool", then the zonal thermal difference factor (Q_{2t}) will decrease during this period. What influence of this unusual thermal state will produce on WPSH? We make the following calculation: Set $Q_{1t} = Q_1 \cdot \sin(\frac{2\pi}{T} \cdot t)$ and $Q_{2t} = Q_2 \cdot [\sin(\frac{2\pi}{T} \cdot t) \cdot 0.7 + \sin(\frac{4\pi}{T} \cdot (t - 50)) \cdot 0.4]$, where Q_{1t} is a normal annual heat variation, and Q_{2t} is a short-period heating disturbance superposed in Q_{1t}, which is adopted to reflect the seasonal thermal abnormality produced by the West Pacific SST abnormal variation in summer of 1998. Take $Q_{3t} = Q_3 = 0.1$, $T = 360$ days, and the thermal pattern is shown in Fig.9, where Q_{2t} has an evident decay in July and August (the 90th–120th model days), and the weakening period is 1–2 months earlier than that of the normal year, which represents such an influence induced by the rapid warming of the West Pacific warm pool during the transition course of El Nino / La Nina. When the stationary heat sources in Eqs. (3)–(5) are replaced by the variable heat sources Q_{1t}, Q_{2t}, and the model is integrated for 360 days, then the variation pattern of the corresponding component of ψ versus heat source is shown in Fig. 10.

Comparing Fig. 8 with Fig.10, it shows that mode 3 (ψ_3) hardly changes and, mode 1 (ψ_1) slightly decays during July–August (the 90th–120th model days), mode 2 (ψ_2), however, has an outstanding change: a stable positive-value state existed in the normal year is transformed into an evident decay state of abnormal year during July–August, which reflects that the stream (geopotential) field of mode 2 is extremely sensitive to the zonal heat source abnormality. It is suggested that it is the abnormal decay of Q_{2t} in midsummer that induces the geopotential field weakening and WPSH retreating southward. Under this condition, taking Fig.5 as an initial field, the geopotential field simulated by the model during June–July (the 75th model day) is similar with that under the condition of the normal seasonal heat source (WPSH is all strong under both conditions), but after a cycle decay of Q_{2t} during July–August, in comparison to the corresponding period condition of normal seasonal heat source, a remarkable variation takes place for the intensity and the range of WPSH in August (the 120th model day), compared with its original extent and intensity in June–July, the central values of WPSH have deeply weakened and the range of central isoline has withdrawn southward. This suggests that it was the abnormality of Q_{2t} during July–August of 1998 that resulted in the relevant WPSH abnormality: its intensity was weakened and its position was withdrawn southward.

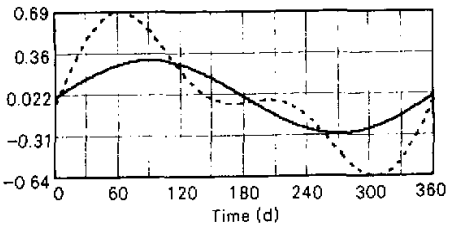

Fig. 9. The seasonal abnormal heat source pattern (—Q_{1t},– – –Q_{2t}).

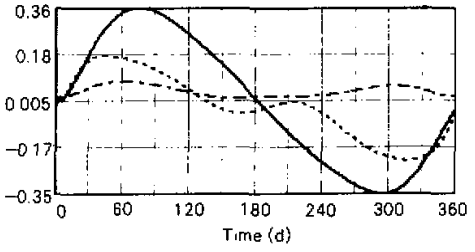

Fig. 10. The numerical integral of seasonal heat source abnormality (—ψ_1,– – –ψ_2,– · –ψ_3).

7. Brief summary

Summing up the above discussion, the important factors that influence the geopotential (stream) field over the subtropical area and consequently induce WPSH variation and medium–range movement are the solar heating (Q_{1t}) and the thermal difference between sea and land (Q_{2t}), the former mainly brings about a gradual variation of the stream (geopotential) field over the subtropical area, being a gradual–variation factor, Q_{1t} induces WPSH slowly moving northward / southward with the seasonal heating or cooling; when the thermal difference between sea and land increases gradually and reaches its critical value, the latter likely results in a catastrophe of the stream (geopotential) field over the subtropical area, being a catastrophic factor, Q_{2t} induces WPSH a smart change (northward–jump). For the medium–range advance / retreat and the abnormal movement of WPSH over the East Asian mainland in the summer, Q_{2t} is a chief forcing term, which expresses such a restriction and influence exerting on WPSH medium–range advance / retreat induced by the thermal difference between the largest mainland (East Asian mainland) and the largest ocean (the Pacific) in summer. It is the lead / restriction effect produced by the vast thermal factor that results in WPSH a marked advance / retreat movement over the East Asian mainland in summer. Therefore, to study and predict WPSH movement, great effort should be concentrated on analyzing the thermal state of both the East Asian mainland and the West Pacific area, especially, the thermal abnormality of the East Asian mainland forcing term (including solar radiation sensible heat and cumulus convection latent heat) and the West Pacific warm pool likely results in WPSH abnormality or catastrophe, which is basically in agreement with another research results (Yu et al., 1991 and Zhang et al., 1995).

Because the adopted model is fairly simple, only some qualitative discussions are made, and there possibly exist some differences between the discussion results and the actual observational facts, but the chief characteristics of the WPSH medium–range movement in summer have basically been described, moreover, the research results are likely useful for further study.

REFERENCES

Charney, J.G., and J.G., De Voro, 1979: Multiple flow equilibria in the atmosphere and blocking. *J. Atmos. Sci.*, **36**, 1205–1216.

Liu Chongjian, and Tao Shiyan, 1983: Subtropical high jump northward and CUSP catastrophe. *Science in China (B).*, **5**, 474–480. (in Chinese)

Miao Jinhai, and Ding Minfang, 1985: The catastrophe and seasonal variation of atmospheric equilibrium state under thermal forcing, subtropical high jump northward. *Science in China (B)*, **1**, 87–96 (in Chinese).

Yu Shihua, and Yang Weiwu, 1991: The features of the subtropical monsoon circulation cell and its relationship with summer circulation over East Asia. *Quarterly Journal of Applied Meteorology*, **2**, 242–247 (in Chinese).

Zhang Ren, and Shi Hansheng, and Yu Shihua, 1995: A non-linear stability study of Western Pacific subtropical high. *Scientia Atmospherica Sinica*, **19**, 687–700 (in Chinese).